

Low-Tortuous Single-Particle-Layer Electrode for High-Energy Lithium-Sulfur

Batteries

Shuo Feng^{1,2}, Rajesh Kumar Singh¹, Yucheng Fu⁵, Zhuo Li^{3,4}, Yulong Wang^{3,4}, Jie Bao¹, Zhijie Xu⁵, Guosheng Li¹, Cassidy Anderson¹, Lili Shi¹, Yuehe Lin², Peter G. Khalifah^{3,4}, Wei Wang¹, Jun Liu¹, Jie Xiao¹, and Dongping Lu^{1,*}

¹Energy and Environmental Directorate, Pacific Northwest National Laboratory, Richland, WA, USA.

²School of Mechanical and Materials Engineering, Washington State University, Pullman, WA, USA.

³Department of Chemistry, Stony Brook University, Stony Brook, NY, USA.

⁴Department of Chemistry, Brookhaven National Laboratory, Upton, NY, USA.

⁵Physical and Computational Science Directorate, Pacific Northwest National Laboratory, Richland, WA, USA.

Table S1. Calculation results of electrode porosity and energy density at different porosities.

Porosity	72%	63%	52%	45%
Thickness (μm)	120	90	70	60
Areal (cm^2)	1.26	1.26	1.26	1.26
Electrode Volume (cm^3)	0.0151	0.0113	0.00882	0.00756
Sulfur loading (mg/cm^2)	4	4	4	4
Sulfur Volume (cm^3)	0.00241	0.00241	0.00241	0.00241
NKB Volume (cm^3)	0.000694	0.000694	0.000694	0.000694
CNF Volume (cm^3)	0.000434	0.000434	0.000434	0.000434
PAA Volume (cm^3)	0.00063	0.00063	0.00063	0.00063
Pore/electrolyte Volume (μl)	10.9	7.16	4.64	3.38
Electrolyte weight (mg)	11.9	7.87	5.1	3.71
Specific capacity (mAh g^{-1})	1000	1000	1000	1000
Total Capacity (mAh)	5.04	5.04	5.04	5.04
Volumetric capacity (mAh cm^{-3})	330	440	566	661
Gravimetric Capacity (mAh g^{-1})	640	640	640	640

Table S2. Electrolyte volume distribution in Li-S cells under flooded electrolyte condition and lean electrolyte condition

Porosity	Inside of Cathode	E/S 10 (total 50 μL) Outside of Cathode	E/S 4 (total 20 μL) Outside of Cathode
72%	10.9	39.1	9.1
63%	7.16	42.8	12.8
52%	4.64	45.3	15.3
45%	3.38	46.6	16.6

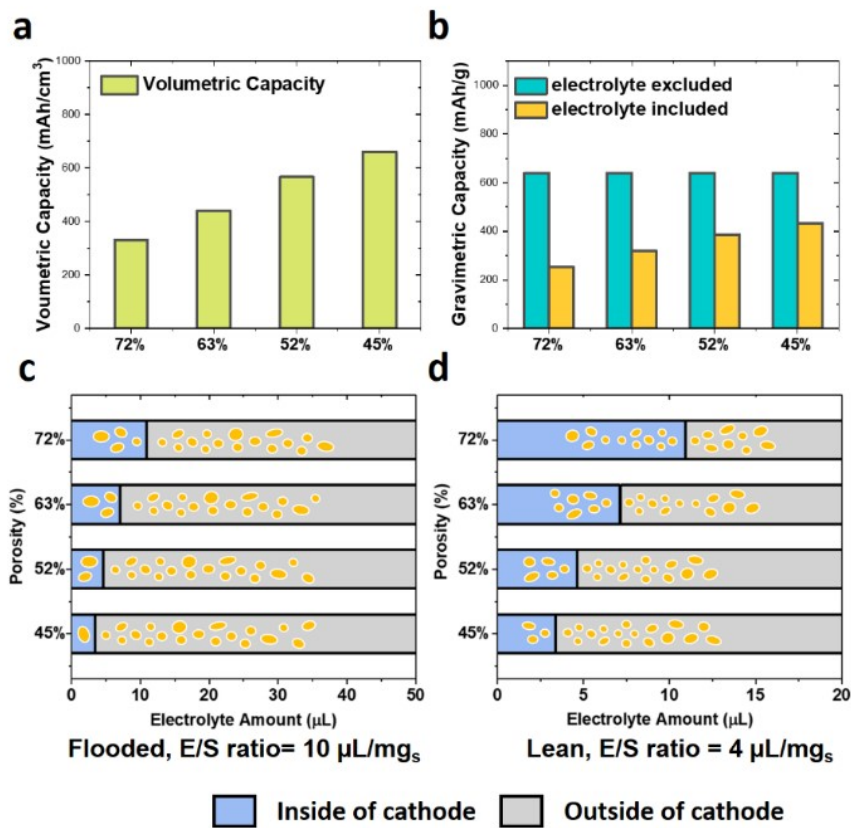


Figure S1. Correlations between a cathode's porosity and its (a) volumetric capacity and (b) gravimetric capacity. Electrolyte distribution in a Li-S cell under (c) flooded and (d) lean electrolyte conditions at various electrode porosities. The detailed calculations are listed in supporting information, Table 1

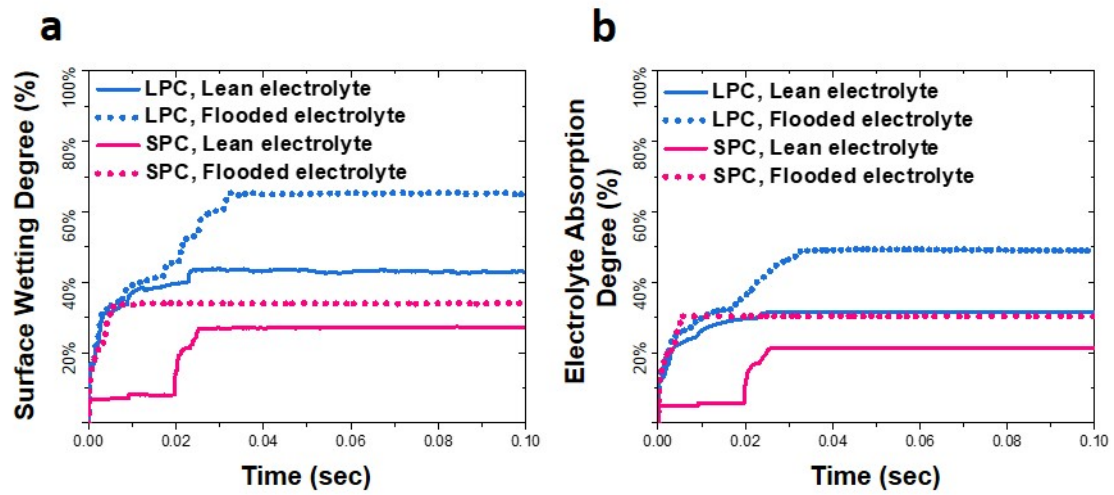


Figure S2. (a) Surface wetting degree and (d) electrolyte absorption degree in LPC and SPC at steady state.

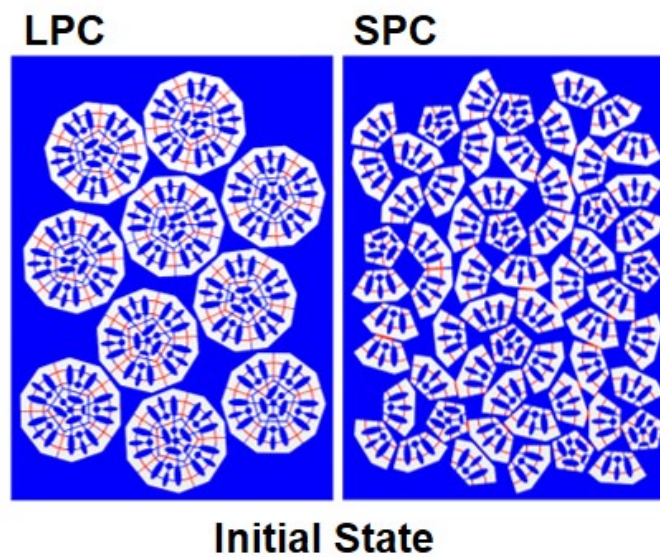


Figure S3. Initial State of polysulfides migration simulation

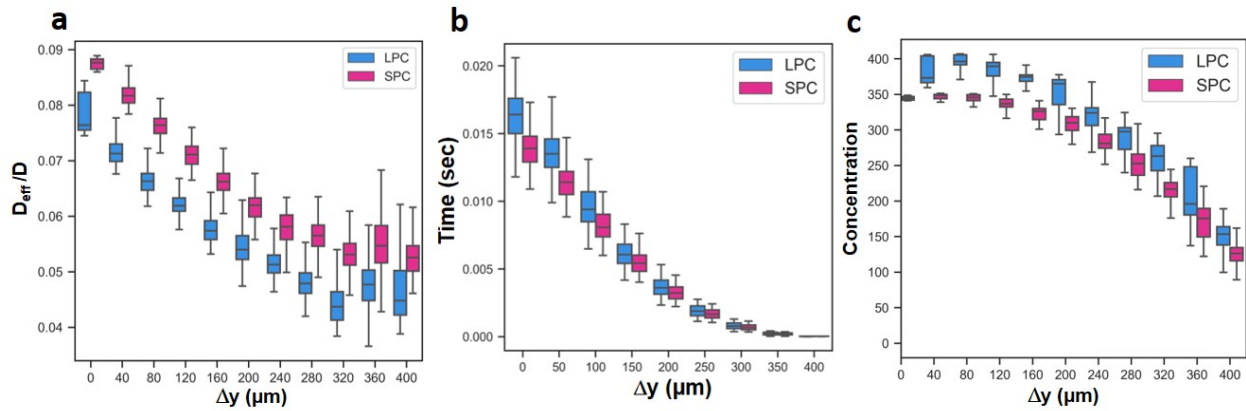


Figure S4. (a) LPS normalized diffusivity at different depths of LPC and SPC at steady state (b) the time of polysulfides diffusing out of the electrode (c) LPS concentration of LPC and SPC at different depths of LPC and SPC at steady state.

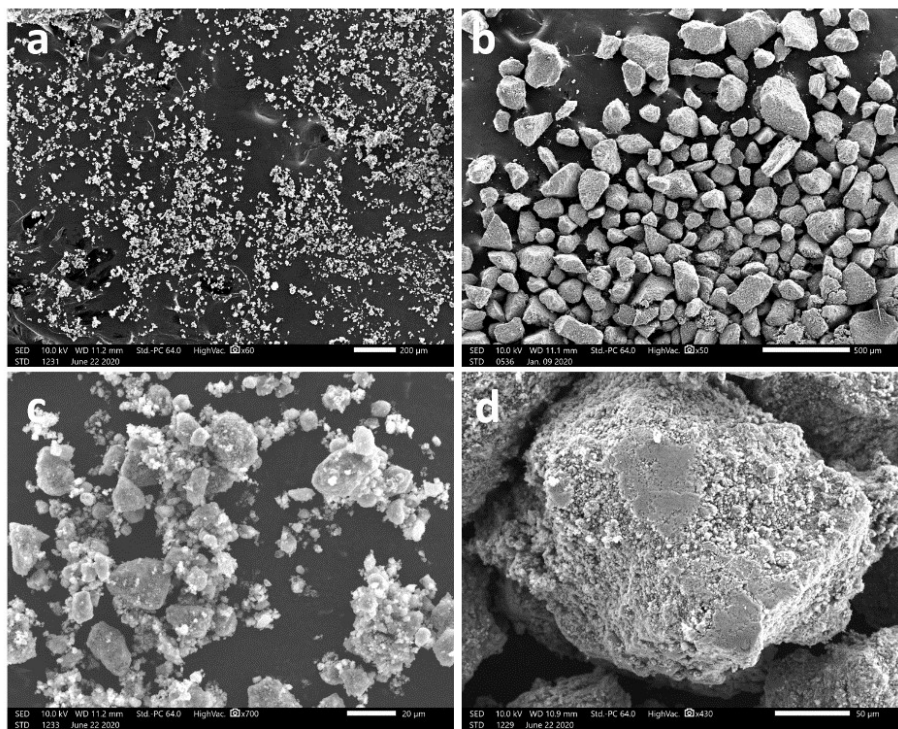


Figure S5. SEM images of small (a, c) and large (b, d) IKB/S particles.

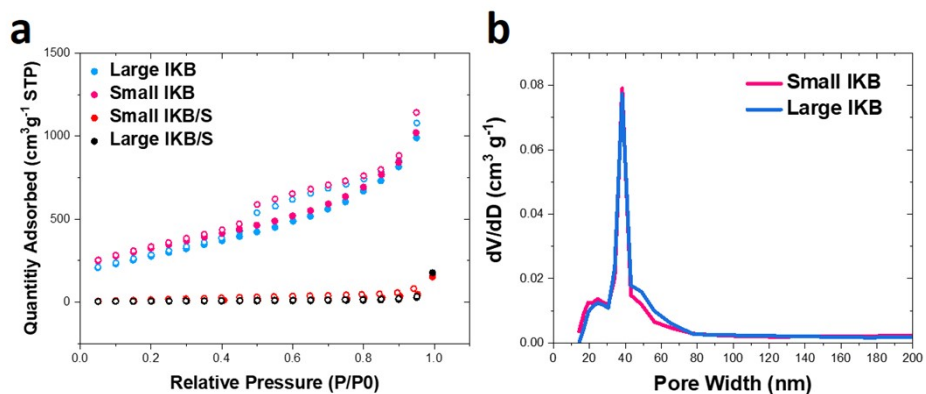


Figure S6. (a) BET adsorption–desorption measurements of small and large IKB particles before and after sulfur infusion. (b) pore size distribution of small and large IKB.

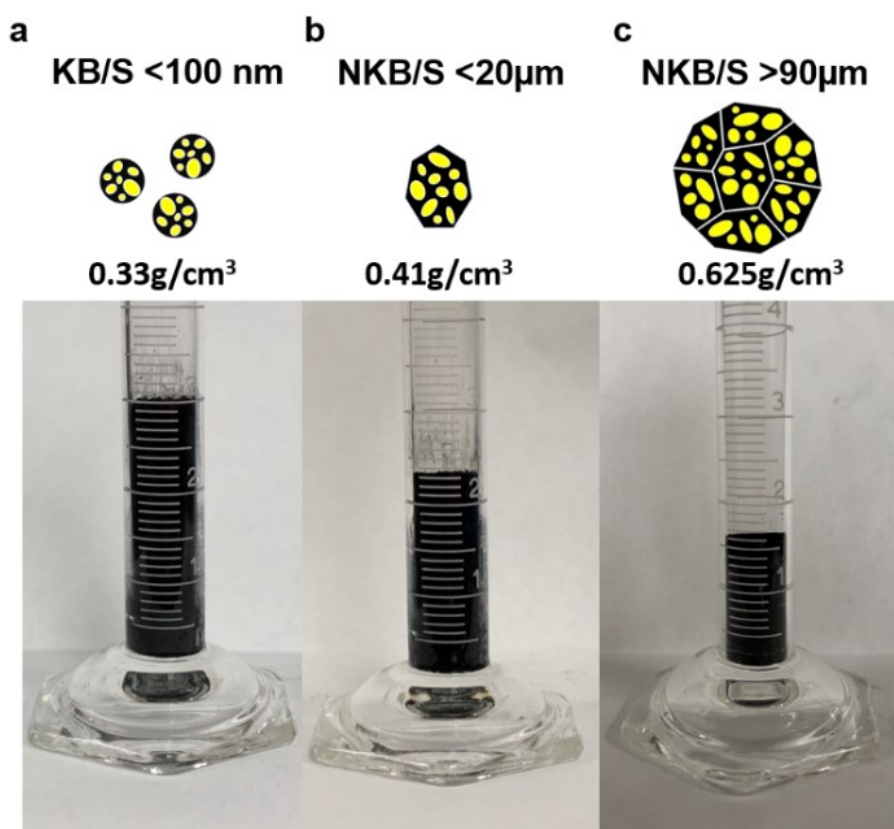


Figure S7. Tap densities of (a) original KB/S composite, (b) small IKB/S particles and (c) large IKB/S particles

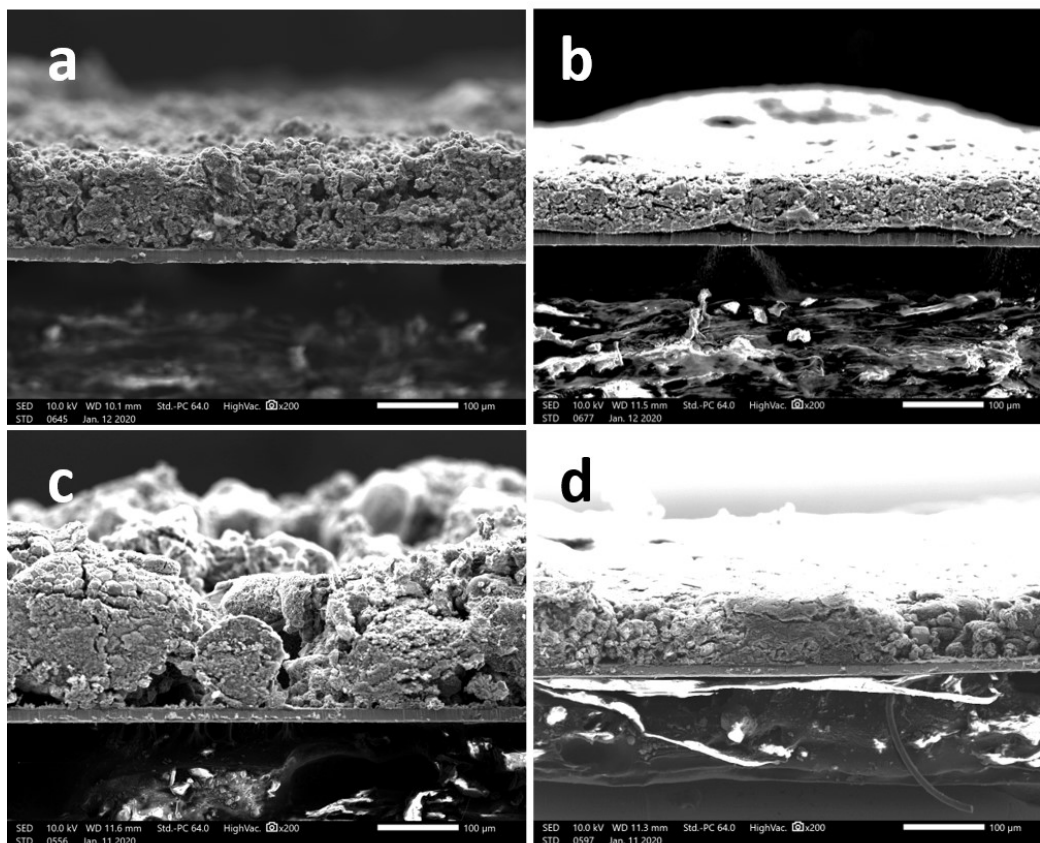


Figure S8. SME images of original (a) SPC, (c) LPC and 45% porosity (b) SPC, (d) LPC, respectively

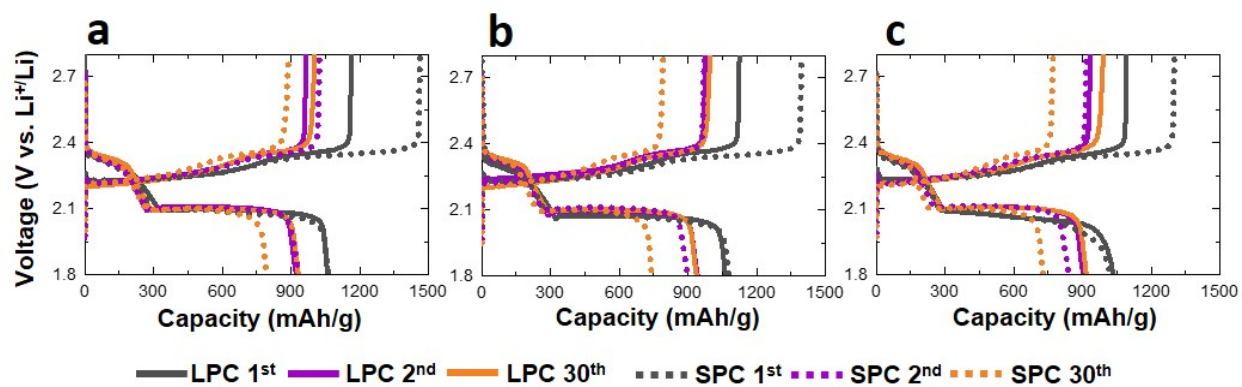


Figure S9. Discharge and charge curves of LPC and SPC under flooded electrolyte condition at 0.1 C, at 62%, 53% and 45% porosity respectively.

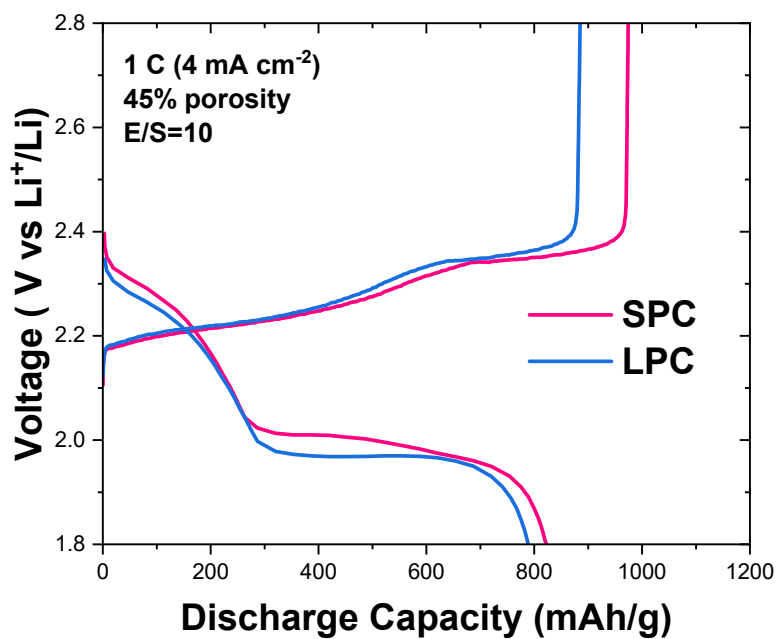


Figure S10. Typical discharge and charge curves of SPC and LPC at 1 C.

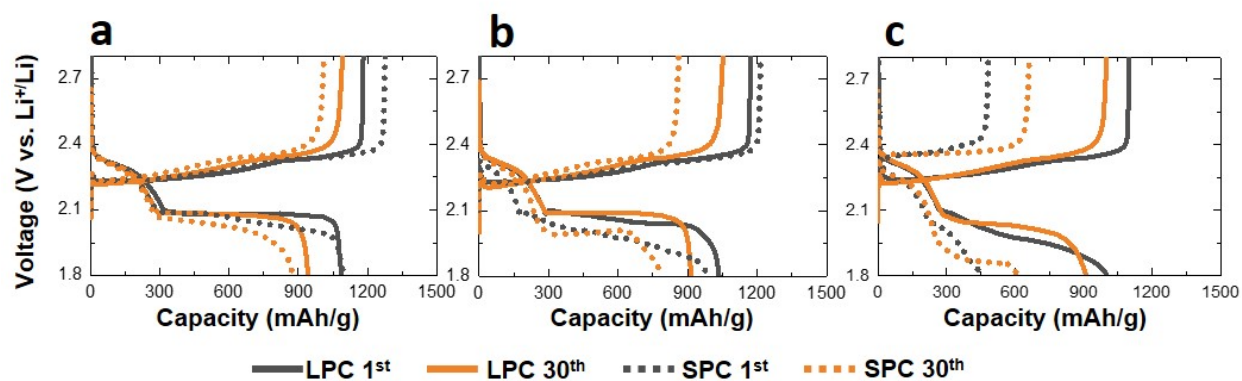


Figure S11. Discharge and charge curves of LPC and SPC under lean electrolyte condition at 62%, 53% and 45% porosity respectively.

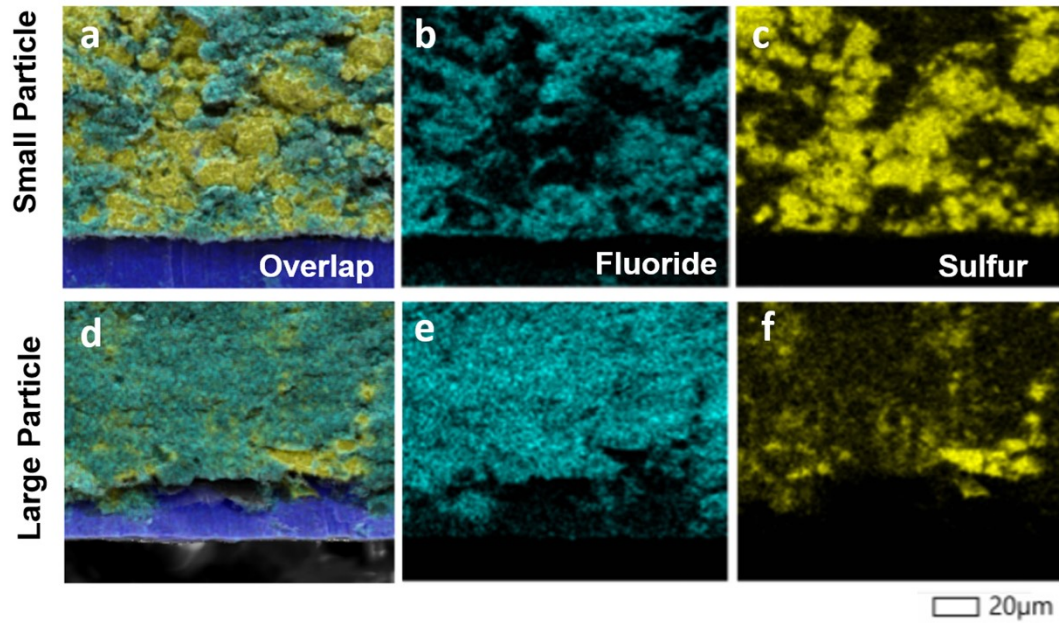


Figure S12. Electron dispersive x-ray spectroscopy of SPC (a-c) and LPC (d-f) after contacting with 1M LiTFSI/DOL/DME.

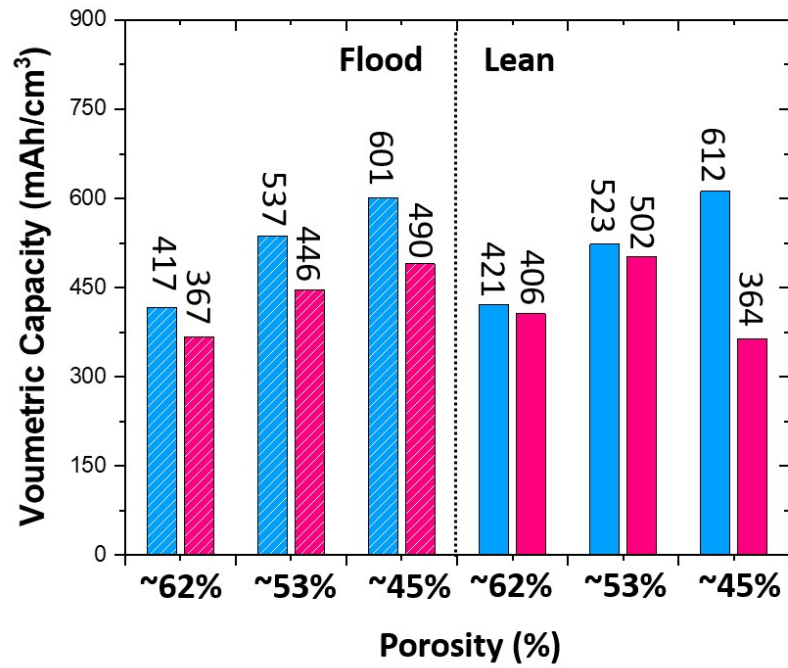


Figure S13. Volumetric capacity of SPC (pink) and LPC (blue) under flood and lean electrolyte conditions at each porosity.

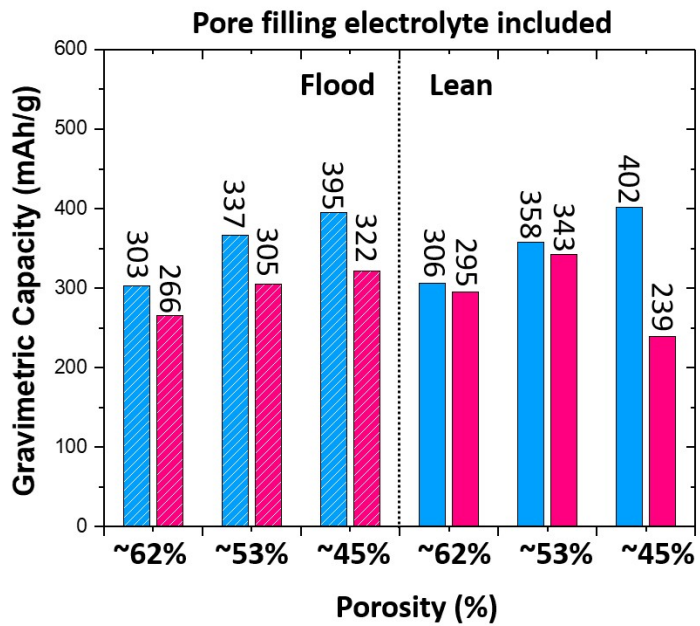


Figure S14. CSC of SPC (red) and LPC (blue) under flood and lean electrolyte conditions at each porosity.

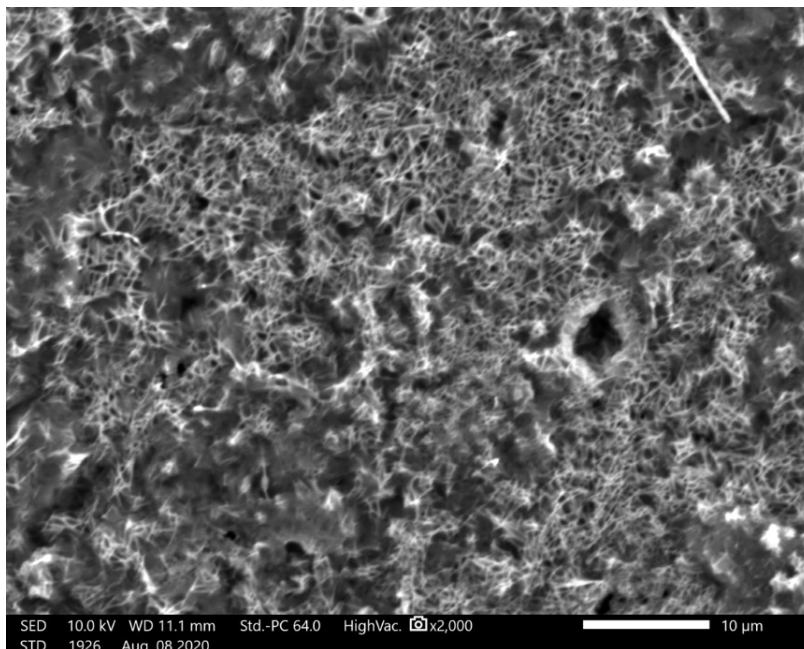


Figure S15. High magnification SEM images of Li_2S on the SPC

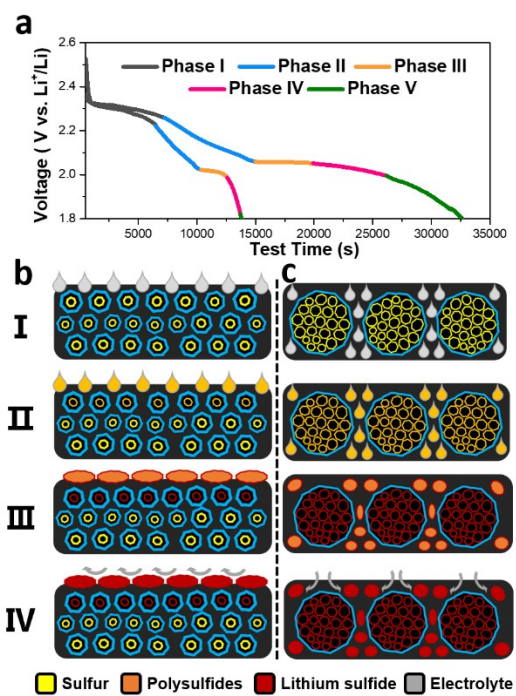


Figure S16. A mechanism illustration depicting the difference of reaction process between LPC and SPC.



Figure S17. Photograph of sample package used in synchrotron characterization.

